Functional Metal Carbides

DOI: 10.1002/anie.201001626

Biotemplating of Metal Carbide Microstructures: The Magnetic Leaf**

*Zoë Schnepp, Wen Yang, Markus Antonietti, and Cristina Giordano**

Biological microstructures display an unparalleled degree of complexity that has long been a source of inspiration for both artists and scientists.[1] In the burgeoning field of materials synthesis, these fascinating structures have been employed as templates to create exquisite replicas from a variety of metal oxides[2] and noble metals.[3] But these are not merely curiosities. By incorporating features of the biological structure, such as porosity, high surface area, or even cellular function,[4] the properties of the ceramic can be modified or enhanced. Remarkably, although biotemplating techniques are well-established in oxide synthesis, there are few corresponding routes to metal carbide materials. Previous work, pioneered by Greil et al.,[5] has focused primarily on the creation of SiC ceramics from precarbonized biological structures and liquid or gaseous silicon. Herein, we present a significant advance on these methods. Using aqueous iron salts, we demonstrate the one-step synthesis of intricate, hierarchical microstructures of magnetic iron carbide (Fe_3C) from a leaf skeleton. We also demonstrate the homogeneity of this conducting Fe_3C network by using the leaves as electrodes for water splitting and electrodeposition of platinum.

Metal carbides offer a range of unique properties that are not available to their oxide counterparts.[6] As such, they have found applications as diverse as hard coatings,[7] medical implants,[8] and catalysis.[9] Iron carbide in particular is more magnetic than iron oxide,[10] chemically resistant, and owing to the fact that it is a metallic conductor, a favorable choice for electrode applications. However, the synthesis of carbide materials can offer numerous challenges and so synthesis routes often involve multiple steps, decomposition of a complex starting material,[11] or synthesis temperatures above 1000 °C.[12] Furthermore, there are few reported routes for controlling the morphology or microstructure of metal carbides compared to the array of methods available for oxide synthesis.

The structural network of veins of a leaf contains bundles of vessels and fibers that are responsible for mechanical strength and also the distribution of water and nutrients to the photosynthetic cells. These vascular bundles are particularly well-suited as a biotemplate for ceramic synthesis because they are rich in lignin.[13] This complex and abundant biopolymer is resistant to degradation and, as a composite with cellulose, provides vascular plants with mechanical strength. The softer tissue surrounding the vessels in leaves can be digested quite easily, leaving the lignin-rich skeleton behind. In this method, the leaf skeleton acts as both a template and a carbon source for formation of the iron or iron carbide material by carbothermal reduction of iron(II) precursors. These networks could find applications as lightweight magnetic materials or electrodes, but more importantly, this method offers a general new route to multiple metal carbide microstructures with improved transport pathways. To be more specific, a leaf is an evolutionarily optimized structure with respect to lightweight design for mechanical stability, offering a maximal transport from and to an area through a hierarchical tubing system. In the present context, it does not matter if these are metabolites or electrons.

To prepare magnetic microstructures, leaf skeletons were vacuum infilled with aqueous iron acetate, blotted to remove excess liquid, and dried at 40 °C in air. On heating to 700 °C under nitrogen, the leaf skeleton turned black but retained the complete network-like structure. The resulting leaf replica was strongly attracted to a permanent magnet (Figure 1 a). Powder X-ray diffraction (pXRD) confirmed the presence of iron carbide (Fe_3C) as a primary crystalline phase in the sample (Figure 1 b), with additional peaks corresponding to metallic iron and graphite. Preliminary investigations of the system suggested that the crystalline composition of the product depended on reaction temperature and time, and also on the precursor. For example, holding the sample for a longer time at the maximum reaction temperature resulted in an increased Fe:Fe_3C peak ratio in the XRD (Supporting Information, Figure S1). This observation is consistent with previous reports of the decomposition of Fe_3C to Fe on sustained heating. Furthermore, changing the iron precursor from $Fe(CH_3CO_2)_2$ to $Fe(NO_3)_3$ lead to the formation of almost phase-pure iron (Supporting Information, Figure S2).

Scanning electron microscopy (SEM) images revealed that the vascular microstructure of the original leaf had been replicated with remarkable accuracy. Figure 2 shows bundles of tubular structures characteristic of xylem, the water transport vessels of plants. In fact, multiple cellular structures, including helical, pitted, and scalariform xylem could be identified. Higher-resolution SEM images of the sample suggested a uniform granular structure both on surfaces and fractured cross-sections (Figure 2 e).

Preparation of the magnetic leaves in an inert atmosphere provides an environment in which the lignocellulose structure of the original biological template is carbonised, releasing CO and/or CO_2. In previous reports of metal carbide biotemplating, this is carried out as a distinct step, the resulting carbon structure then in-filled with for example liquid or gaseous silicon or silicon precursors.[14] Here, however, we used an aqueous metal salt to create an even coating of the metal

[*] Dr. Z. Schnepp, Dr. W. Yang, Prof. M. Antonietti, Dr. C. Giordano
Max Planck Institute of Colloids and Interfaces
Research Campus Golm, 14424 Potsdam (Germany)
Fax: (+49) 331-567-9502
E-mail: pape@mpikg-golm.mpg.de

[**] The authors thank the BASF Company and the Max Planck Society for financial support.

Supporting information for this article is available on the WWW under http://dx.doi.org/10.1002/anie.201001626.

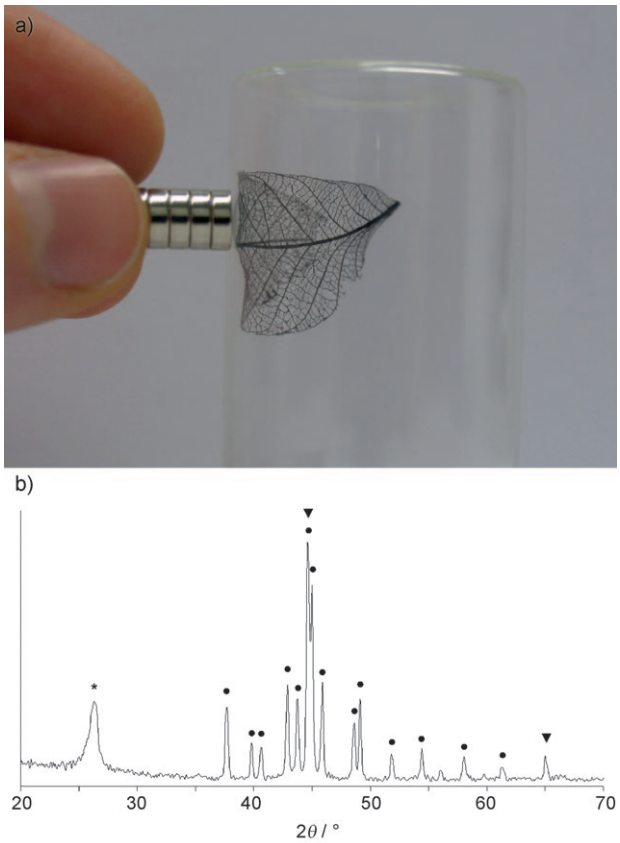

Figure 1. a) Magnetic replica of a rubber fig (*Ficus elastica*) leaf attracted by a permanent magnet; b) powder X-ray diffraction pattern of leaves synthesized from $Fe(CH_3CO_2)_2$, showing peaks for Fe_3C (●, ICDD 04-010-7474), Fe (▼, ICDD 04-008-1441), and graphite (⋆, ICDD 01-075-1621).

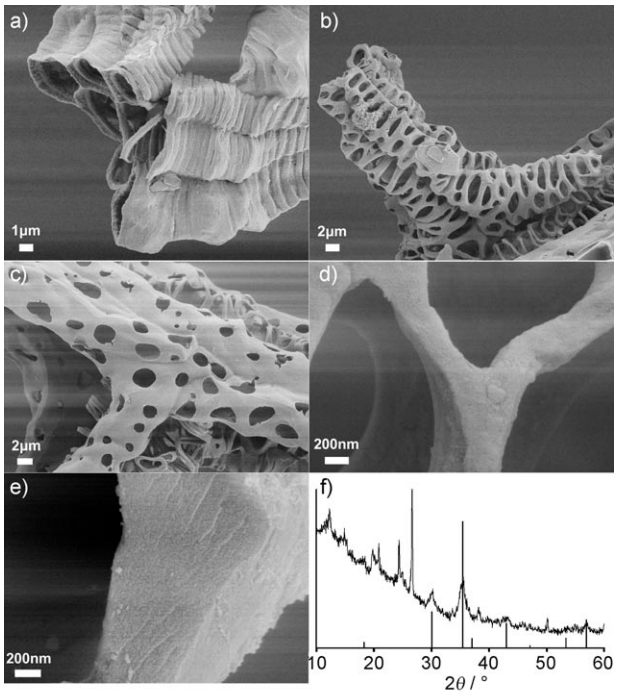

Figure 2. SEM images of the magnetic sacred fig (*Ficus religiosa*) leaf replica, showing a) helical, b,d,e) scalariform, and c) pitted structures characteristic of xylem vessels. f) Powder X-ray diffraction pattern of the structure quenched at 500 °C, with marked peaks corresponding to Fe_3O_4 (ICDD 2010, 04-011-5952). The unmarked peaks did not match any patterns on the ICDD database and probably correspond to a complex mixture of iron intermediate compounds resulting from decomposition of the leaf biopolymers in the presence of iron.

precursor over the original biological template. On heating, the metal and biological precursors simultaneously decompose, producing a series of intermediate iron compounds, including Fe_3O_4 (Figure 2 f). The carbon-rich decomposed leaf skeleton then induces carbothermal reduction of the iron intermediates. In this way, we believe it is possible to form a uniform Fe_3C phase over the entire leaf network.

Fe_3C is exceptional in that it displays high magnetic saturation, stability, and metallic conductivity. By investigating the electrode properties of the leaf, we were therefore able to determine the distribution of metallic Fe_3C over the structure. Carbide leaves were connected at the base to copper wires using electrical solder. This "chimera" was then dipped in an aqueous Na_2SO_4 solution containing phenolphthalein for water electrolysis (Supporting Information, Figure S3). Bubbles formed at both the anodic leaf and the platinum cathode and the solution around the cathode turned deep purple, indicating rise in pH (Figure 3 a,b). This result is consistent with electrolytic water splitting, with production of hydrogen at the cathode and simultaneous release of OH^- ions ($2H_2O + 2e^- \rightarrow H_2 + 2OH^-$). The solution around the leaf anode remained colorless, indicating a lower pH, consistent with the release of oxygen and concurrent formation of H^+ ions ($2H_2O \rightarrow O_2 + 4H^+ + 4e^-$). It should be

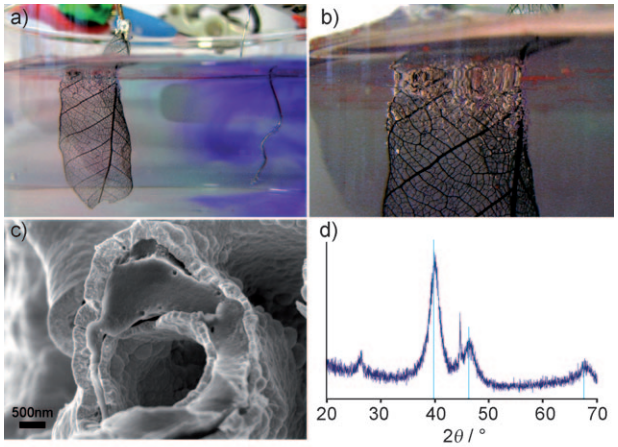

Figure 3. a) Image of the electrolysis experiment, showing bubbles forming around both electrodes; b) a close-up of the leaf anode. The purple color in (a) is phenolphthalein and indicates the release of hydroxide ions concurrent with the formation of hydrogen at the platinum cathode. The lack of color around the leaf anode is consistent with the formation of oxygen and a drop in pH. c) An SEM image of a leaf vessel, showing a layer of electrodeposited platinum; d) powder X-ray diffraction pattern of the sample in (c) with marked peaks corresponding to platinum.

underscored that the production of oxygen often passivates or destroys all non-noble nanostructured anodes, whereas oxygen production from the Fe_3C leaf was sustained for 1 hour without visibly slowing. The appearance of the electrode was unchanged (Supporting Information, Figure S4).

In a second set of experiments, the lower half of the leaf was then immersed in a $K_2[PtCl_4]$ solution containing a platinum counter-electrode and a voltage applied across the cell. The immersed section of the leaf turned a light grey color and bubbles were formed at the platinum anode, suggesting electrodeposition of platinum on the leaf cathode. SEM of the samples showed a homogeneous layer over the entire immersed leaf section (Figure 3c), which increased in thickness when a higher concentration of $K_2[PtCl_4]$ was used for electrodeposition (Supporting Information, Figure S5a,b). Control samples, dipped in $K_2[PtCl_4]$ solution for the same time without an applied voltage, showed a thinner and considerably less homogeneous coating, consistent with autoreduction of platinum (Supporting Information, Figure S5c,d). PXRD of a powdered sample of electroplated leaf showed large, broad peaks that are characteristic of platinum, giving an approximate particle diameter, by the Scherrer equation, of 4 nm (Figure 3d). Transmission electron microscopy (TEM) showed clusters of nanoparticles (ca. 5 nm), with energy dispersive X-ray analysis (EDXA) confirming peaks for platinum (Supporting Information, Figure S6). Importantly, these data are consistent with a homogeneous conducting Fe_3C phase over the whole leaf network.

In summary, we have prepared iron carbide replicas of a leaf skeleton. By dispersing the iron precursor in solution form over the template, the microstructure of the leaf veins has been replicated with remarkable accuracy. Significantly, the full structure of the leaf was intact after the heating procedure. By demonstrating the use of these materials as electrodes for water splitting and the electrodeposition of platinum, we showed that a homogeneous coating of Fe_3C has been achieved over the whole structure. The importance of magnetic leaf replicas lies not just in their intrinsic beauty and as a proof-of-principle, but as a general procedure for biological templating of metal carbide materials. This method has great promise for the simple synthesis of a variety of microstructured objects for catalytic and electrochemical purposes.

Experimental Section

An iron(II) acetate precursor solution was prepared by dissolving $Fe(CH_3CO_2)_2$ (10% by weight) in deionized water. Similarly, an aqueous iron(III) nitrate ($Fe(NO_3)_3$, 50% by weight) precursor solution was prepared. Leaf skeletons prepared from leaves of the rubber fig (*Ficus elastica*) and sacred fig (*Ficus religiosa*) were soaked in the iron precursor solutions under vacuum until all bubbling had ceased. The leaves were then drained, blotted to remove excess liquid, and dried in air at 40°C. Samples were calcined under a flow of nitrogen at 2°C/min to 700°C and cooled to room temperature. Electrodes were prepared by fixing ceramic leaves to sections of copper wire with electrical solder. For electrolysis of water, a solution of Na_2SO_4 (0.5% by weight) was prepared containing a few drops of phenolphthalein pH indicator solution. The leaf electrode was connected to a circuit as the anode with a platinum cathode. Both electrodes were dipped into the Na_2SO_4 solution, and a potential of 5 V was applied across the cell. For platinum deposition, the electrode was connected as the cathode to a cell with a platinum counter-electrode and Ag | AgCl | KCl reference electrode. The cell was filled with $K_2[PtCl_4]$ solution (1 mM or 5 mM) so that the lower half of the ceramic leaf was in contact with the solution. A voltage of 200 mV was applied for 600 s before the leaf was removed, washed three times with deionized water, and dried at 40°C.

Received: March 18, 2010
Revised: July 6, 2010
Published online: August 16, 2010

Keywords: biotemplates · electrodes · iron carbide · magnetic properties · microstructures

[1] S. Mann, *Biomineralization: Principles and Concepts in Bioinorganic Materials Chemistry*, Oxford University Press, Oxford, **2001**.
[2] S. R. Hall, *Biotemplating*, World Scientific, London, **2009**.
[3] a) K. M. Bromley, A. J. Patil, A. W. Perriman, G. Stubbs, S. Mann, *J. Mater. Chem.* **2008**, *18*, 4796–4801; b) A. Sugunan, P. Melin, J. Schnürer, J. G. Hilborn, J. Dutta, *Adv. Mater.* **2007**, *19*, 77–81.
[4] H. Zhou, X. Li, T. Fan, F. E. Osterloh, J. Ding, E. M. Sabio, D. Zhang, Q. Guo, *Adv. Mater.* **2010**, *22*, 951–956.
[5] A. Zampieri, W. Schwieger, C. Zollfrank, P. Greil in *Handbook of Biomineralization: Biomimtic and Bioinspired Chemistry* (Eds.: P. Behrens, E. Baeuerlein), Wiley-VCH, Weinheim, **2007**, p. 255.
[6] S. T. Oyama, *The Chemistry of Transition Metal Carbides and Nitrides*, Chapmann and Hall, London, **1996**.
[7] D. Garg, P. N. Dyer, D. B. Dimos, S. Sunder, *J. Am. Ceram. Soc.* **1992**, *75*, 1008–1011.
[8] M. Brama, N. Rhodes, J. Hunt, A. Ricci, R. Teghil, S. Migliaccio, C. Della Rocca, S. Leccisotti, A. Lioi, M. Scandurra, G. DeMaria, D. Ferro, F. R. Pu, G. Panzini, L. Politi, R. Scandurra, *Biomaterials* **2007**, *28*, 595–608.
[9] N. Ji, T. Zhang, M. Zheng, A. Wang, H. Wang, X. Wang, J. G. Chen, *Angew. Chem.* **2008**, *120*, 8638–8641; *Angew. Chem. Int. Ed.* **2008**, *47*, 8510–8513.
[10] L. J. E. Hofer, E. M. Cohn, *J. Am. Chem. Soc.* **1959**, *81*, 1576–1582.
[11] H. Song, X. Chen, *Chem. Phys. Lett.* **2003**, *374*, 400–404..
[12] P. G. Li, M. Lei, W. H. Tang, *Mater. Res. Bull.* **2008**, *43*, 3621–3626.
[13] R. F. Evert, *Esau's Plant Anatomy*, 3rd ed., Wiley-Interscience, **2006**, p. 69.
[14] H. Sieber, *Mater. Sci. Eng.* **2005**, *412*, 43–47.

